

Dynamical decoupling and recoupling of the Wigner solid to a liquid helium substrateDavid G. Rees ^{1,*}, Sheng-Shiuan Yeh,^{1,*} Ban-Chen Lee,^{1,*} Simon K. Schnyder ², Francis I. B. Williams,^{3,4} Juhn-Jong Lin ^{1,5,6,*} and Kimitoshi Kono ^{7,5,8,†}¹*NCTU-RIKEN Joint Research Laboratory, Institute of Physics, National Chiao Tung University, Hsinchu 300, Taiwan*²*Fukui Institute for Fundamental Chemistry, Kyoto University, Kyoto 606-8103, Japan*³*Laboratoire de Physique des Solides, Universite Paris-Sud, 91405 Orsay, France*⁴*Institute for Solid State Physics and Optics, Wigner Research Centre for Physics, Budapest H-1121, Hungary*⁵*RIKEN CEMS, Wako 351-0198, Japan*⁶*Department of Electrophysics, National Chiao Tung University, Hsinchu 300, Taiwan*⁷*International College of Semiconductor Technology, National Chiao Tung University, Hsinchu 300, Taiwan*⁸*KFU-RIKEN Joint Research Laboratory, Institute of Physics, Kazan Federal University, Kazan, 420008 Russia*

(Received 25 May 2020; accepted 11 August 2020; published 24 August 2020)

We investigate the dynamical interaction between an electron crystal trapped above the surface of liquid helium and surface waves ('rippplons') excited by its motion. At rest, the electron system is 'dressed' by static ripplons to form 'ripplopolaron' states. As the electrons move, resonant ripplon scattering results in a growth of the riplopolaron effective mass, on timescales comparable with the inverse of the ripplon frequency (~ 100 ns). Under sufficient driving force, the electron system decouples from the surface waves and moves at high velocity, before decelerating sharply when the electron solid and surface excitations recouple to form a 'new' riplopolaron system. The mass of the newly formed riplopolarons is similar to that in the initial static case.

DOI: [10.1103/PhysRevB.102.075439](https://doi.org/10.1103/PhysRevB.102.075439)**I. INTRODUCTION**

At low temperatures, surface-state electrons (SSEs) trapped above liquid helium substrates self-organize to form a triangular lattice, the classical Wigner solid (WS) [1,2]. One intriguing result of this spatial ordering is a spontaneous deformation of the helium surface below, as the electrostatic pressure exerted by each electron on the liquid results in the formation of an array of shallow 'dimples' (dimple lattice, DL) commensurate with the electron lattice [3]. The coupled electron-dimple system is analogous to polaronic states formed in crystal lattices in which electrons deform the surrounding lattice structure and become self-trapped [4–6]. Just as the polaron state can be viewed as an electron dressed by virtual phonons, the surface electron lattice can be described as being dressed by quantized capillary waves, or 'rippplons'; the complex formed by each surface electron and its accompanying dimple is therefore termed as a 'ripplopolaron' [7,8].

Upon applying an electric field parallel to the helium surface, the electron and dimple lattices move together. However, when the force is sufficiently strong, the electrons can decouple from the dimples and move freely across the helium surface [9]. Similar decoupling processes can be observed for solid-state polarons, although at picosecond timescales [10]. In contrast, riplopolaron dynamics can be investigated in real time using straightforward transport measurements because

the timescale of the helium surface response is naturally much longer than that of an ordinary solid; for capillary waves with wavelength comparable to the spacing between electrons in the Wigner solid, the inverse of the ripplon frequency is typically 10–100 ns.

We have previously reported a novel 'stick-slip' type of electron motion in which the electron solid repeatedly decouples from, and then recouples to, the dimple lattice [11]. When the driving voltage is smoothly ramped, the velocity of the electron solid is initially limited by Bragg-Cherenkov (BC) ripplon scattering, in which ripplons generated by the moving electrons interfere constructively with the dimple lattice, resonantly increasing the dimple depth and the drag force exerted on the electron solid [12,13]. Because the electron velocity becomes fixed to the coherent ripplon phase velocity during this resonant scattering phase, the driving electric field acting on the electron system grows over time, eventually reaching the threshold for WS-DL decoupling. The electron lattice then escapes the trapping potential formed by the dimples and moves with low resistance. However, the resultant sudden flow of charge causes a rapid reduction in the driving force, allowing the electron solid to recouple to the surface dimples. If the driving voltage is ramped continuously this stick-slip cycle is repeated, leading to spontaneous oscillations in the electron current.

This stick-slip behavior was investigated for surface electrons confined in a microchannel device. By confining the electron system in a long, narrow channel, the driving electric field and the surface electron density (and so the current density) can be precisely controlled and are highly homogeneous. The channel confinement was typically several tens of the

*Present address: Cryogenic Ltd, 6 Acton Park Estate, The Vale, London W3 7QE, United Kingdom.

†kkono@nctu.edu.tw

electron lattice constant in width. For the classical quasi-1D electron lattices investigated here, in which the system width is comparable with the interparticle spacing, the positional order of the electron system can fluctuate rapidly due to the thermally-driven formation of lattice defects [14,15]. This results in the increased motion of electrons about their equilibrium lattice sites and so fluctuations in the strength of the WS-DL coupling. For repeated measurements, the decoupling of the electron lattice from the dimple lattice is therefore found to occur over a range of values of the driving force and so at different points in time as the driving voltage is ramped. This behavior is analogous to thermally activated escape from the zero-voltage state in current-biased Josephson junctions [16].

For slow voltage ramps, the stochasticity in the WS-DL decoupling can smooth the observed average current signal, obscuring the true transport behavior [17]. In this report however, this effect is negated by the use of rapid, steplike voltage ramps that pre-empt the escape by thermal fluctuation and synchronize it with the applied stimulus. This technique allows accurate measurement of the surface electron current during the WS-DL decoupling and recoupling processes. Thus we are able to study in detail the dynamical increase of the DL depth when the electron system is driven at the resonant velocity, the electron motion in the decoupled state, and the conditions under which the moving electron system can recouple to the helium surface.

The report is arranged as follows; in Sec. II we describe the experiment in detail. In Sec. III we examine the response of the electron solid to the steplike voltage stimulus and identify an anomalous transport regime in which the electrons travel at a limiting velocity despite being decoupled from the dimple system. In Sec. IV we investigate the dynamics of the decoupling and recoupling processes in more detail. In Sec. V we draw our conclusions.

II. EXPERIMENT

The sample [Fig. 1(a)] is the same as that used in previous studies [11,15]. The device consists of a system of $2.2\ \mu\text{m}$ -deep microchannels that are filled with liquid helium by capillary flow. These microchannels are arranged to form left and right electron reservoirs, each comprised of some 25 parallel microchannels. The microchannel boundary is defined both geometrically and electrostatically by the guard electrode, which lies in the plane of the helium surface. A dc bias of 0 V was applied to electrodes beneath the helium in the left and right reservoirs, which we denote the left and right reservoir electrodes, respectively. In order to confine electrons within the reservoirs, a dc bias of $-0.2\ \text{V}$ was applied to the guard electrode. The reservoirs are separated by a central microchannel (hereafter referred to simply as the channel) that is $7.5\ \mu\text{m}$ wide and $l = 100\ \mu\text{m}$ long. Electrons were confined in the channel by dc biases applied to electrodes beneath the helium (bottom gate) and at the channel boundary (split gate); these voltages are denoted V_{bg} and V_{sg} , respectively.

Surface electrons were generated by thermionic emission from a tungsten filament positioned above the sample. To drive electron transport between the reservoirs, through the channel, a transient voltage V_{lr} , applied to the left reservoir

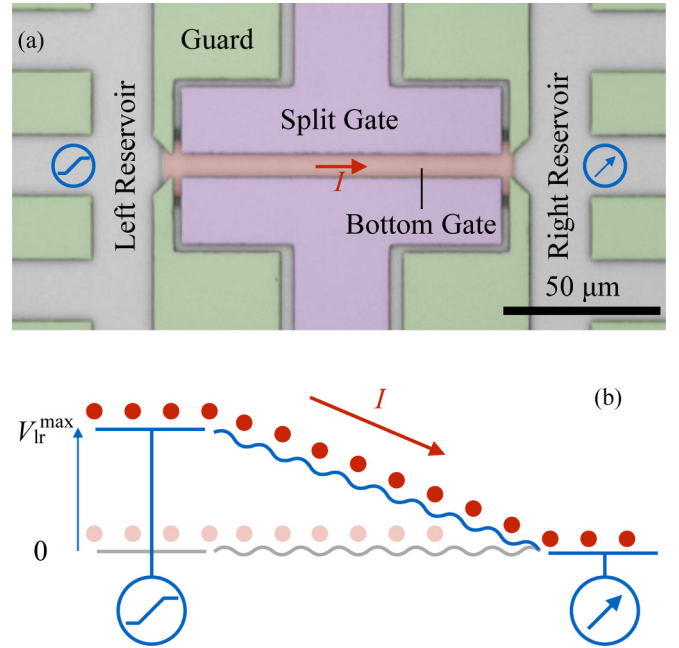


FIG. 1. (a) False-color optical image of the central microchannel, as described in the text. (b) Schematic of the transport measurement. V_{lr} is ramped quickly to V_{lr}^{max} establishing a potential gradient E_x along the channel. Current then flows, inducing a displacement current in the right reservoir electrode, until electrostatic equilibrium is restored. If E_x is large enough the electrons can escape the dimple surface profile.

electrode, was ramped to a value V_{lr}^{max} in a time t_r . (In the limit $t_r = 0$ the driving voltage is stepped discontinuously). The surface electron current I was obtained by measuring the displacement current induced in the right reservoir electrode using a transimpedance preamplifier with rise time 100 ns, and a digital storage oscilloscope. The signal was averaged over several thousand V_{lr} cycles. A correction was made to allow for the fraction (22%) of the displacement current that flows to electrodes other than the right reservoir electrode [11]. When I changes faster than the rise time, the amplifier output can overshoot by some 10% of the true amplitude change but then settles within $\sim 300\ \text{ns}$.

Finite element modeling was used to calculate the effective width of the electron sheet in the channel w_e , its average areal electron density n_s , and so the average linear electron density $n_l = w_e n_s$ [18,19]. The SSE velocity along the channel was then calculated as $v_e = I/en_l$. The variation of the driving electric field as electrons move through the channel is given by $E_x(t) = [V_{lr}(t) - Q(t)/2C]/l$. Here $Q(t)$ is the charge transferred between the reservoirs, calculated by integration of the current signal, and $C = 1.01\ \text{pF}$ is the capacitance between each reservoir electrode and the electron system [11].

For the measurements reported here, the temperature was 0.6 K. Under these conditions, the electron systems in the reservoir regions, which are kept at low density, remain liquid. In this case, due to the lack of long range order in the electron system, and a thermal velocity for the free electrons that greatly exceeds the phase velocity of ripples that dress the static electron lattice, no riplopolarons form and the

electrons remain highly mobile. The electron density in the channel can be controlled independently of these regions; by increasing V_{bg} , the electron density in the central channel can be increased until the WS forms. At $T = 0.6$ K, the electron system should form a Wigner solid when $n_s \approx 7.1 \times 10^{12} \text{ m}^{-2}$ [20–23]. This is satisfied for $V_{bg} = 0.18$ V. We note that the electron densities investigated here generally exceed the limit found for ‘bulk’ surface electron systems in quasi-infinite geometry ($n_s \approx 2 \times 10^{13} \text{ m}^{-2}$). This is because the electrohydrodynamic instability that causes the electron system to ‘break through’ the bulk liquid is suppressed by the microstructuring of the helium surface [24,25].

The resonant Bragg-Cherenkov scattering occurs when the electron velocity v_e becomes equal to the phase velocity v_{ph} of ripples whose wave vector coincides with the first reciprocal lattice vector of the electron lattice. The first reciprocal lattice vector is given by $G_1 = 2\pi(2/\sqrt{3})^{1/2}n_s^{1/2}$. For the electron systems investigated here, with typical surface densities of $\sim 10^{13} \text{ m}^{-2}$, the BC resonance occurs for $v_e = v_{ph} = \sqrt{\sigma G_1/\rho} \sim 10 \text{ m s}^{-1}$, where σ and ρ are the surface tension and density of liquid helium, respectively.

III. TRANSPORT IN THE COUPLED AND DECOUPLED REGIMES

In Fig. 2 we show the surface electron current flowing in response to a voltage step for which $V_{lr}^{\max} = 25$ mV and $t_r = 100$ ns, as shown in Fig. 2(a). When the electron density and the perpendicular electric field that presses the electrons against the helium surface, E_z , are low (low V_{bg}) we expect relatively weak coupling between the electron system and the ripples. Indeed, as shown in the inset to Fig. 2(b), for the lowest value of $n_s = 0.78 \times 10^{13} \text{ m}^{-2}$ ($V_{bg} = 0.2$ V) the electron velocity greatly exceeds v_{ph} ($\sim 10 \text{ m s}^{-1}$) when the voltage step is applied, and then follows an exponential-like decay, as expected for a linear RC circuit. However, as the electron density and pressing electric field increase, plateaulike structures develop in the current response. The main panel in Fig. 2(b) shows the current response for higher electron densities; in the range $4.12 \times 10^{13} \leq n_s \leq 5.93 \times 10^{13} \text{ m}^{-2}$ ($1.60 \text{ V} \leq V_{bg} \leq 2.35 \text{ V}$) the electron velocity still initially exceeds v_{ph} when the voltage is stepped, but then settles on a plateau at a velocity close to 160 m s^{-1} . We denote this plateau velocity as v_{pl} . After moving at v_{pl} for several μs the electron system decelerates sharply to v_{ph} , signaling that at this point the Wigner solid recouples to the helium surface. After the recoupling, the WS-DL system continues to move for several more μs until electrostatic equilibrium between the two reservoirs is reached and the current becomes zero.

For the highest values of the electron surface density $n_s \geq 6.05 \times 10^{13} \text{ m}^{-2}$ ($V_{bg} \geq 2.60$ V) the strong pressing electric field results in the formation of deep dimples from which the electrons cannot escape under the applied driving field (these dimples are further deepened by BC scattering). The electron system therefore always remains coupled to the dimple lattice. Note that for the intermediate range $5.93 \times 10^{13} \text{ m}^{-2} \leq n_s \leq 6.05 \times 10^{13} \text{ m}^{-2}$ the stochasticity of the WS-DL decoupling results in the decoupling occurring for only a fraction of the

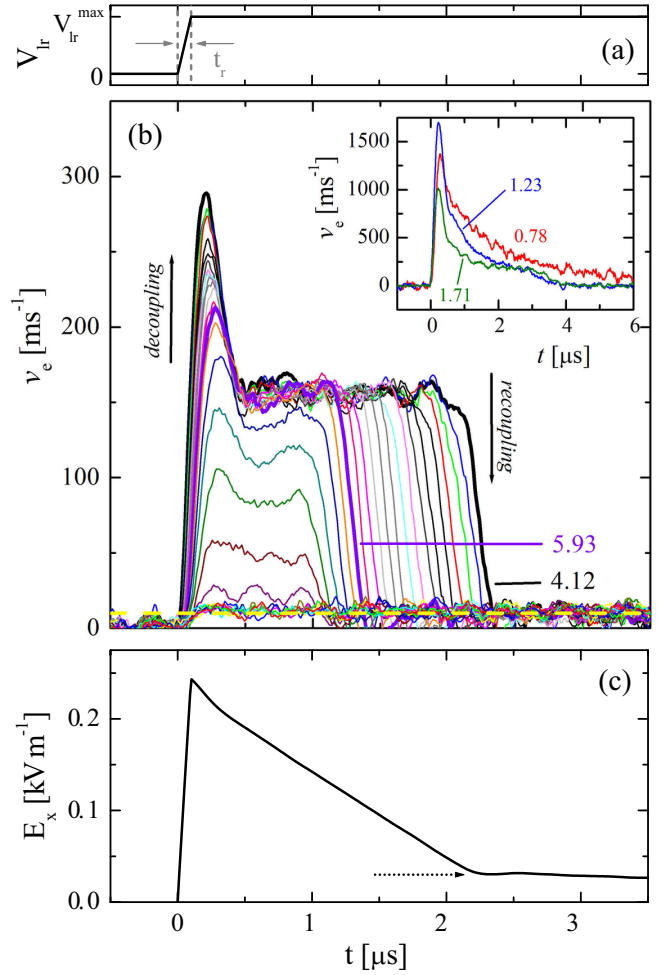


FIG. 2. (a) Schematic of the driving voltage pulses used to investigate the ripplopolaron decoupling and recoupling. V_{lr} is stepped from 0 to V_{lr}^{\max} in a time t_r . (b) v_e against t for values of V_{bg} from 1.6 to 3.0 V ($n_s = 4.12 \times 10^{13}$ to $7.48 \times 10^{13} \text{ m}^{-2}$) increased in 50 mV steps. Curves for $n_s = 4.12 \times 10^{13} \text{ m}^{-2}$ and $n_s = 5.93 \times 10^{13} \text{ m}^{-2}$ are labeled. Here $V_{lr}^{\max} = 25$ mV and $t_r = 100$ ns. The dashed line indicates the typical electron velocity for BC scattering $v_e = 10 \text{ m s}^{-1}$. The apparent smooth decrease of the height of the velocity plateau, between the high velocity and BC scattering regimes, is an artifact of averaging over many measurements in which the WS-DL decoupling occurs probabilistically, as explained in the text. The inset shows v_e against t for lower values of n_s , as labeled in units of 10^{13} m^{-2} . (c) E_x against t for $n_s = 4.12 \times 10^{13} \text{ m}^{-2}$. The arrow marks the value of E_x^{re} .

voltage cycles. The average signal amplitude therefore varies smoothly between v_{pl} and v_{ph} as V_{bg} is increased [17].

The observations of the quasiexponential current decay at low electron densities and the limitation of the electron velocity due to Bragg-Cherenkov scattering at high electron densities are as expected. However, the appearance of a high-velocity plateau is a novel nonlinear effect. Remarkably, the electron velocity remains constant in this plateau regime despite the decreasing driving force, which decreases linearly as electrons flow at a constant rate between the reservoirs [Fig. 2(c)]. Because this behavior clearly develops as the

electron density and pressing field increase it can be attributed to an interaction between the electron system and the helium substrate. However, the interaction mechanism in this velocity regime remains unclear; for $v_{ph} \approx 200 \text{ m s}^{-1}$ the corresponding ripplon wavelength approaches the atomic scale, and is much shorter than the electron de Broglie wavelength for an electron of temperature 0.6 K, and so BC scattering should not be expected to occur. We therefore consider other mechanisms that may result in the high-velocity plateaus. Over several experimental runs v_{pl} was always found to lie within the range $150\text{--}225 \text{ m s}^{-1}$ (although no systematic dependence on temperature or other experimental parameters could be determined, and the velocity was always consistent during each run). This velocity range lies close to, but below, the speed of first sound in liquid helium (238 m s^{-1}). This suggests that the electron motion may be limited by a strong drag force as it approaches the phonon velocity barrier. However, in this high velocity regime it is not clear how the interaction between the electron solid and phonons in the liquid below can give rise to such an effect. One possibility is that the motion of a *macroscopic* deformation of the helium surface below the electron crystal is limited by an increasing drag force as its velocity approaches the phonon barrier [26]. In this model, no dependence of v_{pl} on n_s would be expected, as is observed.

Nonlinear effects due to electron heating also play an important role in the decoupled transport regime. For a free electron system subjected to the large driving fields used here, electron temperatures of order 1000 K have been predicted [27,28]. In this regime the electron solid will melt, and transitions to and between higher subbands for the electron motion perpendicular to the helium surface will occur, resulting in a quasi-3D electron system and a strongly modified response to the driving field. However, a self-consistent calculation of the heating and resulting nonlinear conductance of the electron system goes beyond the scope of this report. We conclude that, under large pressing and driving fields, the interaction between the electron system and the helium substrate remains strong even when the electron system is decoupled from the dimples. This results in highly nonlinear transport behavior.

IV. DECOUPLING AND RECOUPLING DYNAMICS

We turn to the dynamics of the WS-DL decoupling and recoupling. The use of short voltage steps allows us to probe the dynamical response of the helium surface to the electron motion before the decoupling occurs. This is achieved by setting the value of t_r and then varying the value of V_{lr}^{\max} to find the threshold voltage at which the electron system decouples from the dimple lattice. We define this threshold as the value of V_{lr}^{\max} for which the average current signal rises above the v_{ph} plateau. The corresponding values of the threshold electric field, E_x^{de} , are shown in Fig. 3(a), for four values of n_s . As expected, the decoupling threshold is generally higher for higher n_s because the increased pressing electric field creates a deeper dimple lattice from which the electron system must escape. E_x^{de} also increases with t_r , indicating that the dimple depth increases over time when the system is driven at velocities approaching the BC resonance.

With decreasing t_r the decoupling threshold extrapolates to a finite value, which is higher for more positive n_s . In

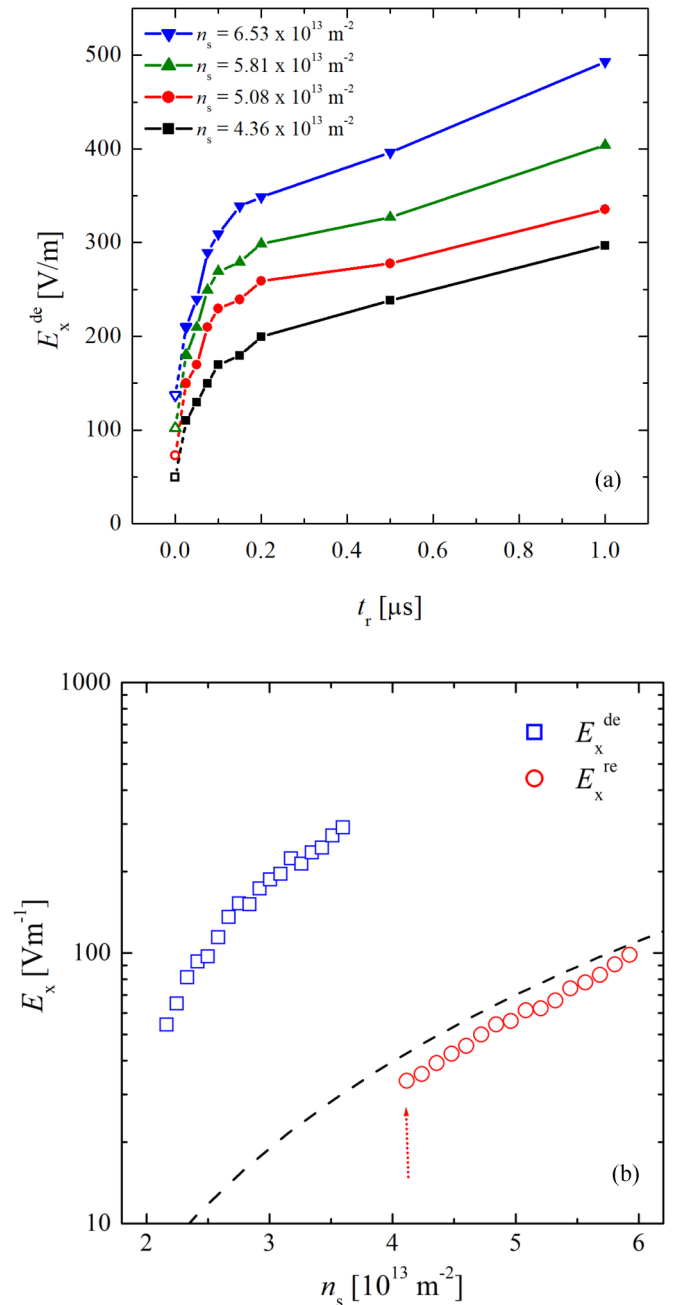


FIG. 3. Dynamical response of the helium substrate to the Wigner solid motion. (a) E_x^{de} against t_r for different values of n_s . The open points represent the decoupling threshold for static ripplons calculated using the simple hydrostatic treatment of the WS-DL interaction described in the text. (b) E_x^{de} for the case in which BC scattering proceeds for several tens of μs before decoupling occurs and values of E_x^{re} taken from the data presented in Fig. 2(b), against n_s . The dashed line indicates the trapping threshold for the shallow DL profile predicted by the hydrostatic model. The arrow indicates the data point extracted from the measurement shown in Fig. 2(c).

this limit, the BC scattering does not deepen the dimples, and the threshold values therefore represent the driving field required to decouple the electron system from the dimples that are formed when the system is at rest. For this static

case, the surface deformation profile can be estimated using a hydrostatic model which gives the dimple depth as $\xi_0 = \sqrt{3eE_z \exp(-W)/8\pi^2\sigma}$, where e and $\exp(-W)$ are the elementary charge and the self-consistent Debye-Waller factor, respectively [3,29]. Assuming a sinusoidal surface profile, the electric field required to decouple the electron system from the dimple deformation can then be estimated as $E_x^{de} = \xi_0 E_z (2\pi/a)$, where a is the interelectron separation. These calculated thresholds are shown in Fig. 3(a). The measured values of E_x^{de} extrapolate back to those calculated for the static WS-DL system with good accuracy confirming that the hydrostatic model gives a good description of the interaction between the static electron solid and the liquid helium surface.

E_x^{de} increases most rapidly during the initial ~ 200 ns of driving confirming that the dimple depth, and so the hydrodynamic mass of the WS-DL system, increase significantly during this period. We consider this timescale for the dimple growth to be reasonable as the resonant ripplon frequencies involved for BC scattering are of order 100 MHz. Over longer timescales the dimple depth continues to increase slowly, indicating that a steady equilibrium is not achieved during the measurement time. This could be a result of damping of the BC resonance, due to factors such as the electron thermal motion [14] or ripplon decay [30], which might suppress the rate of increase of the dimple depth.

After the decoupling, the driving electric field drops at a constant rate as electrons move through the channel at v_{pl} . Then, at a certain threshold field which we denote E_x^{re} , the electron velocity drops sharply signaling that the electron system couples once again to the surface dimples. Values of E_x^{re} , taken from the transport measurements shown in Fig. 2(b) for $4.12 \times 10^{13} \leq n_s \leq 5.93 \times 10^{13} \text{ m}^{-2}$, are shown in Fig. 3(b). Also shown is the static decoupling threshold field calculated using the hydrodynamic model. The experimental values fall close to this line. We also show values of E_x^{de} recorded using smooth voltage ramp measurements similar to those described in Ref. [11]. In these measurements the BC resonance was observed to proceed for some tens of μs , allowing the dimple depth to approach its saturated value, before the decoupling occurred. Although recorded at lower electron densities and pressing electric fields (lower V_{bg}), the values of E_x^{de} clearly exceed those of E_x^{re} , due to the increased depth of the DL under the BC resonance.

The WS-DL recoupling occurs when E_x drops close to the value expected for trapping in the static dimple profile. This suggests that the recoupling occurs due to the formation of a ‘new’ dimple lattice as the helium surface deforms under the pressure by the moving electron lattice. This self-trapping can only occur when E_x is small enough to prevent the electrons immediately escaping the dimples that are formed. Although surface waves on helium decay slowly [30], our measurements indicate that when the waves forming the standing wave dimple lattice configuration are decoupled from the electron lattice and released to propagate freely, the resulting destructive interference leads to a rapid loss of the ‘original’ dimple profile. We expect this to occur on a timescale comparable with the inverse of the ripplon frequency (~ 10 ns).

V. CONCLUSIONS

In summary, we have measured the dynamical motion of an electron solid above a liquid helium substrate during both decoupling from the bound ripplon state and its subsequent recoupling to surface excitations. BC scattering significantly deepens the surface dimples before the decoupling occurs; after the decoupling, the response of the electron solid is highly nonlinear due to unexpectedly strong interactions with the helium substrate. The reformation of the ripplon state can only occur when the driving force becomes low enough to allow the electrons to become trapped in the surface deformation once again, the threshold for which is accurately predicted by a simple hydrostatic model. The dynamics observed here can be compared with those of other polaronic states in which electron self-trapping occurs.

ACKNOWLEDGMENTS

We thank N. R. Beysengulov for finite element modeling and A. O. Badrutdinov, M. I. Dykman, and B. Sas for helpful discussions. This work was supported by the Taiwan Ministry of Science and Technology (MOST) through Grant Nos. MOST 103-2112-M-009-017 and MOST 108-2122-M-009-013. and the MOE ATU Program, and by JSPS KAKENHI Grant Nos. 24000007 and JP17H01145. This work was performed according to the Russian Government Program of Competitive Growth of Kazan Federal University.

-
- [1] C. C. Grimes and G. Adams, *Phys. Rev. Lett.* **42**, 795 (1979).
 - [2] E. Wigner, *Trans. Faraday Soc.* **34**, 678 (1938).
 - [3] Y. P. Monarkha and V. B. Shikin, *JETP* **41**, 710 (1975).
 - [4] A. S. Alexandrov and J. T. Devreese, *Advances in Polaron Physics* (Springer, Berlin, 2010).
 - [5] I. Hulea, S. Fratini, H. Xie, C. Mulder, N. Iossad, G. Rastelli, S. Ciuchi, and A. Morpurgo, *Nat. Mater.* **5**, 982 (2006).
 - [6] M. Koschorreck, D. Pertot, E. Vogt, B. Fröhlich, M. Feld, and M. Köhl, *Nature (London)* **485**, 619 (2012).
 - [7] S. A. Jackson and P. M. Platzman, *Phys. Rev. B* **24**, 499 (1981).
 - [8] M. Saitoh, *J. Phys. Soc. Jpn.* **55**, 1311 (1986).
 - [9] K. Shirahama and K. Kono, *Phys. Rev. Lett.* **74**, 781 (1995); *J. Low Temp. Phys.* **104**, 237 (1996).
 - [10] N.-H. Ge, C. Wong, R. Lingle, J. McNeill, K. Gaffney, and C. Harris, *Science* **279**, 202 (1998).
 - [11] D. G. Rees, N. R. Beysengulov, J.-J. Lin, and K. Kono, *Phys. Rev. Lett.* **116**, 206801 (2016).
 - [12] M. I. Dykman and Y. G. Rubo, *Phys. Rev. Lett.* **78**, 4813 (1997).
 - [13] W. F. Vinen, *J. Phys.: Condens. Matter* **11**, 9709 (1999).
 - [14] G. Piacente, I. V. Schweigert, J. J. Betouras, and F. M. Peeters, *Phys. Rev. B* **69**, 045324 (2004).
 - [15] D. G. Rees, N. R. Beysengulov, Y. Teranishi, C.-S. Tsao, S.-S. Yeh, S.-P. Chiu, Y.-H. Lin, D. A. Tayurskii, J.-J. Lin, and K. Kono, *Phys. Rev. B* **94**, 045139 (2016).

- [16] M. H. Devoret, J. M. Martinis, and J. Clarke, *Phys. Rev. Lett.* **55**, 1908 (1985).
- [17] D. G. Rees, S.-S. Yeh, B.-C. Lee, K. Kono, and J.-J. Lin, *Phys. Rev. B* **96**, 205438 (2017).
- [18] N. R. Beysengulov, D. G. Rees, Y. Lysogorskiy, N. K. Galiullin, A. S. Vazjukov, D. A. Tayurskii, and K. Kono, *J. Low Temp. Phys.* **182**, 28 (2016).
- [19] F. Hecht, *J. Numer. Math.* **20**, 251 (2012).
- [20] J. M. Kosterlitz and D. J. Thouless, *J. Phys. C: Solid State Phys.* **6**, 1181 (1973).
- [21] B. I. Halperin and D. R. Nelson, *Phys. Rev. Lett.* **41**, 121 (1978).
- [22] A. P. Young, *Phys. Rev. B* **19**, 1855 (1979).
- [23] G. Deville, *J. Low Temp. Phys.* **72**, 135 (1988).
- [24] D. Marty, *J. Phys. C Solid State Phys.* **19**, 6097 (1986).
- [25] P. Leiderer, E. Scheer, K. Kono, J.-J. Lin, and D. G. Rees, *J. Low Temp. Phys.* **183**, 258 (2016).
- [26] P. Leiderer, W. Ebner, and V. B. Shikin, *Surf. Sci.* **113**, 405 (1982).
- [27] M. Saitoh, *J. Phys. Soc. Jpn.* **42**, 201 (1977).
- [28] T. Aoki and M. Saitoh, *J. Phys. Soc. Jpn.* **44**, 71 (1978).
- [29] Y. P. Monarkha and K. Kono, *J. Phys. Soc. Jpn.* **74**, 960 (2005).
- [30] P. Roche, G. Deville, K. O. Keshishev, N. J. Appleyard, and F. I. B. Williams, *Phys. Rev. Lett.* **75**, 3316 (1995).